Scientific Research Publishing

Comparative Petro-Geochemistry of the Intrusive Granitoids of the Comoé Basin and the Granitoids of the Ferkessédougou Batholith (Côte D'Ivoire, Man-Leo Shield): Geodynamic Implications for the West African Craton (WAC)

Tokpa Kakeu Lionel-Dimitri Boya[1]*, Allou Gnanzou[1], Aristide Ghislain Beugré Dago[1], Nahoua Silue[2], Koffi Raoul Teha[1], Alain Nicaise Kouamelan[1]

[1]Laboratory of Geology, Mineral and Energy Resources/Training and Research Unit in Earth Sciences and Mineral Resources, Félix HOUPHOUËT-BOIGNY University, Abidjan, Côte d'Ivoire
[2]Ministry of Mines, Petroleum and Energy, Duékoué Regional Directorate, Duékoué, Côte d'Ivoire
Email: *lionelboya2000@yahoo.fr

Abstract

The study of Birimian granitoids is of great importance because it allows us to understand the architecture of the West African crust and the processes that shaped it. In order to contribute to the improvement of knowledge on the geodynamic context of the emplacement of certain granitoids of the West African craton, this article addresses some essential problems of the Birimian, namely distinguishing the real nature of the magmas and the mechanisms that generated this Birimian crust. On the West African craton, there are intrusive granites in volcano-sedimentary furrows, in meta-sedimentary basins and granites that form batholiths separating these structures. To provide an answer to this scientific concern, we conducted a comparative study of the granitoids of the Comoé basin (Tiassalé region) and those of the large batholith of Ferkessédougou (Daloa region). From this study, it appears that these Birimian granitoids have been identified as granites, granodiorites and tonalites in the Tiassalé region while in Daloa, they are assimilated to anatexites and granites. They present very diverse aspects and contexts of emplacement: the granitoids of the Comoé basin have characteristics of type I granite, indicating direct crystallization of mantle magmas in a syntectonic emplacement, while in the Daloa region, some granitoids are magmatic, others migmatitic or metasomatic, reflecting a certain complexity relating to their genesis.

1. Introduction

The West African Craton (**Figure 1**) is a vast complex of Archean and Palaeo-proterozoic terrains with alternating greenstone furrows and large granitoid ba-tholiths.

Greenstone belts or birimic volcano-sedimentary series in West Africa are often intruded by basin-type or belt-type granitoids (Pouclet et al., 1996; Hirdes & Davis, 1998; Pouclet et al., 2006). The surrounding formations of these granito-ids were metamorphosed between 2.2 and 2.0 Ga under greenschist facies condi-tions that can reach amphibolite facies near certain granitoid plutons (Abou-chami et al., 1990; Boher, 1991; Taylor et al., 1992; Hirdes et al., 1996; Pouclet et al., 2006; Lompo, 2010).

For several decades, understanding the geodynamic context of rocks has been the subject of numerous studies. While several authors (Bonhomme, 1962; Tagi-ni, 1971; Feybesse et al., 2006; Pouclet et al., 2006; Vidal et al., 2009) agree that the Eburnean cycle led to the tectonic assembly of the Archean core and the various Paleoproterozoic domains between 2.15 and 2.07 Ga, following the ac-cretion of juvenile crust between 2.25 and 2.15 Ga, the geodynamic evolution of the Paleoproterozoic realm is the subject of one of the main debates.

Indeed, some authors such as Pouclet et al. (2006), Vidal et al. (2009) and Lompo (2010) propose structural models of domes and basins set up by gravity and vertical tectonics during the geodynamic evolution of the Eburnean.

Another stream of researchers composed of Milési et al. (1992), Billa et al. (1999), Feybesse et al. (2006), interprets Eburnean orogenic events as the prod-uct of modern nappe-like tectonics. Transcurrent shear zones, located at the in-terface between greenstone belts and granito-gneissic domains, characterize the late evolution of the Eburnean orogeny (Jessell et al., 2012; Teha, 2019).

From the foregoing, it emerges that despite the different currents of thought relating to the geodynamic context of the placement of the rocks on this craton, the authors are rather unanimous for the placement of these granitoids during the Eburnean cycle between 2.25 and 2.07 Ga. Although they were emplaced during the same orogenic cycle, do their geochemical characteristics place them in the same magmatic lineage or in different lineages? To answer this question, we compare the geochemical characteristics of granitoids from the Tiassalé re-gion emplaced in a basin context with those from the Daloa region on the Ferké batholith.

These birimian granitoids present very diverse aspects and contexts of em-placement (Casanova, 1973). Some are magmatic, others migmatitic or metasomatic.
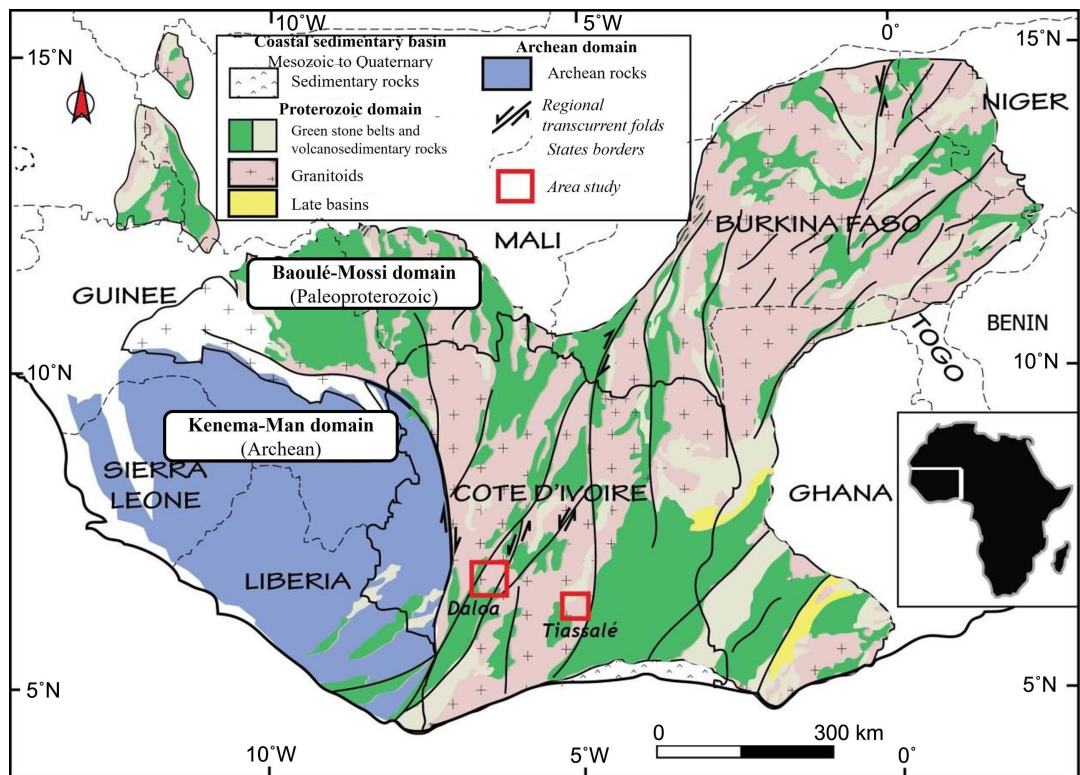
Figure 1. Structural framework of the West African craton and the different study areas (modified from Milesi et al., 2004).

Granitoids emplaced in sedimentary and volcano-sedimentary basins can be distinguished from large batholiths separating volcano-sedimentary furrows.

As the geochemical relationship between inter-fault batholith granitoids and basin-type granites has not yet been studied, this comparison between the granitoids of the Daloa region located on the Ferké large batholith and those of the Tiassalé region located in the Comoé basin is important in characterizing the magmatic sources that generated the West African crust.

2. Regional Geological Setting

2.1. Geology of the Tiassalé Region

The Tiassalé region is located in the southern part of the Comoé Basin (Figure 1) in the Lake District of Côte d'Ivoire. This region is essentially composed of metasedimentary rocks and granitoid intrusions. Previous work on the lithostratigraphy of the Comoé unit shows that it is essentially composed of quartzites, basic to acidic vulcanites (Alric, 1985), shales and sandstones (Arnould, 1961; Alric et al., 1987) resting in discordance on an antebirimic granito-migmatitic basement. Volcanic formations are very little represented and are essentially found at the periphery of the basin. Several granitoid plutons outcrop in the southern part of the Comoé basin. However, other granitoids such as granodiorites and deformed tonalites observed in the basin seem to predate the sedimentary deposits.

2.2. Geology of the Daloa Region

The Daloa region is located in central-western Côte d'Ivoire (Figure 1) in the Baoulé-Mossi domain (Tagini, 1971) at the level of the Ferkessédougou batholith (Ferké). This batholith is a vast granitic unit 400 km long and 50 km wide oriented N-NE8. Studies in the Katiola-Marabadiassa (Doumbia, 1997), Zuénoula and SASCA areas (Ouattara, 1998) have shown the complex character of this batholith formed by small amalgamated plutons.

The Daloa region is essentially made up of granitoids that intrude into meta-sedimentary rocks. The geographical distribution of the different rocks defines a magmatic suite that progressively evolves from migmatites in the north to anatexia granites (Daloa sector) to a southern domain (Issia sector) essentially made up of leucogranites, leucomonzogranites, pegmatites, albitites (Dago et al., 2019).

The detailed study of these granitoids has enabled us to define three major groups: 1) anatexites, whose facies evolve from metatexites to anatexite granites; 2) granites in the strict sense (s. s), which include leucogranites, two-mica granites and leucomonzogranites; and 3) granitic pegmatites and pneutomalytes (Dago et al., 2019).

3. Materials and Methods

Granitoid samples were collected in different regions of Côte d'Ivoire: the one in the region of Daloa in the center-west of Côte d'Ivoire and the others in the region of Tiassalé in the center of the country. For this geochemical study, 24 granitoid samples were selected for comparison between basin granitoids and those constituting the batholiths separating the Birimian furrows.

To define the chemical characteristics of the different rocks, 18 samples representative of the different lithologies encountered in the Daloa region (2 metatexites, 6 diatexites; 2 anatexia granites; 2 two-mica granites and 6 leucogranites) and 6 granitoids from the Tiassalé region were selected for geochemical analysis at Bureau Veritas Commodities Ltd (Vancouver-Canada). The samples were first dried, then crushed and finally pulverized through a 200 μm sieve. The major elements SiO_2, Al_2O_3, Fe_2O_3, CaO, MgO, Na_2O, K_2O, MnO, P_2O_5 and TiO_2 were analyzed by X-ray fluorescence spectrometry (XRF) method with PANalytical Axios FAST multichannel and trace and rare earth elements by optical emission spectrometry (ICP-OES). Loss on ignition was obtained by heating to 1000˚C.

XRF is a chemical analysis technique using a physical property of matter, X-ray fluorescence When we bombard matter with X-rays, the matter re-emits energy in the form, among other things, of X-rays; it is fluorescence X, or secondary emission of X-rays. The spectrum of X-rays emitted by matter is characteristic of the composition of the sample, by analyzing this spectrum, we can deduce the elementary composition, that is- that is, the mass concentrations of elements.

ICP OES is an inductively coupled plasma optical emission spectrometry. It is an instrumental technique based on the separation, identification and quantification of the constituent elements of a sample according to their mass, based on the coupling of a plasma torch generating ions and a mass spectrometer, which separates these ions by mass. Samples are frequently prepared by dissolving, usually in acid, in order to analyze the solution. This is injected into the plasma in the form of a fine aerosol, generated by a pneumatic (nebulizer), ultrasonic or physico-chemical device.

4. Petrographic Characteristics

4.1. Petrographic Facies of Tiassalé

4.1.1. Granite
Granites are found in the southern and central-western parts of the study area. The outcrops encountered at N'Douci and Tiassalé are in the form of multimetric boulders intruding the metasediments. These granites have a normal grainy to micrograined porphyritic texture (Figure 2(a)) and are made up of quartz; plagioclase sometimes in the process of damouritisation or microclinisation, orthoclase; biotite and numerous opaque minerals.

4.1.2. Granodiorite
Granodiorite is present in the Bodo locality. Macroscopic observation of this rock shows a mesocratic color and a grainy texture (Figure 2(b)). Microcline and plagioclase feldspars are the most abundant minerals and are often slightly altered to sericite. Quartz is less abundant than feldspars, with medium-sized grains. The rock also contains amphibole, more precisely green hornblende, which occurs as automorphic rods. Biotite generally forms large patches containing inclusions of quartz, zircon and opaque minerals.

4.1.3. Tonalite
The outcrops occur either as scattered blocks or as slabs. Macroscopically (Figure 2(c)), a number of characteristics bring these formations closer to granodiorites: their mesocratic colour, the richness of quartz, biotite and amphibole. It is sometimes difficult to distinguish between the two types of facies. In thin sections, the samples taken showed a grainy texture, sometimes with a porphyroid tendency.
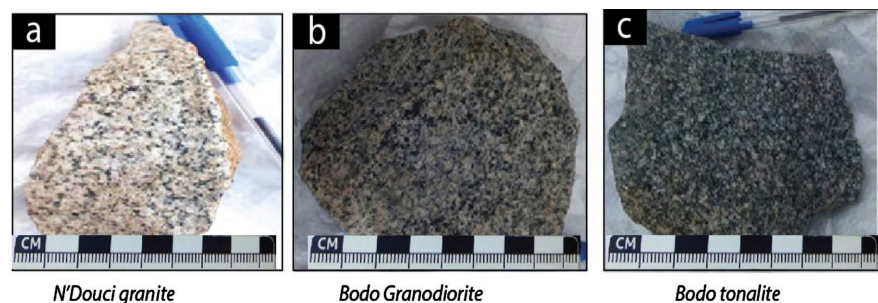

N'Douci granite   Bodo Granodiorite   Bodo tonalite

Figure 2. The Tiassalé region granitoids.

4.2. Petrographic Facies of the Daloa Region

The study area is essentially made up of granitoids that intrude meta-sedimentary rocks. The geographical distribution of the different rocks defines a magmatic sequence that progressively evolves from migmatites in the north to anatexia granites (Daloa sector) to a southern domain (Issia sector) essentially made up of leucogranites, leucomonzogranites, pegmatites, albitites…

The detailed study of these granitoids has enabled us to define three major groups: 1) anatexites, whose facies evolve from metatexites to anatexia granites; 2) granites in the strict sense (s. s), which include leucogranites, two-mica granites and leucomonzogranites; and 3) pegmatites and granitic pneutomalytes.

4.2.1. Anatexites

The anatexites form a continuous sequence from metatexites to anatexia granites (Figures 3(a)-(c)). Depending on the appearance and quantity of the neosome formed, which is itself dependent on the melting rate of the protolith, there is an evolution from metatexites (migmatitic granodiorites), diatexites to anatexia granites. At the outcrop, the migmatites have a ribbon-like appearance and show alternating light and dark beds of variable thickness.

In the so-called anatexia granites, the segregation observed in the migmatites is no longer present. The paleosome has completely disappeared, leading to a pink granite rich in potassium feldspars.

All these rocks have similar mineralogy with a few exceptions. Microscopically, the leucosome is essentially granoblastic and the melanosome lepido-granoblastic. The mineralogical assemblage consists of quartz, plagioclases varying from albite to oligoclase, potassium feldspars often perthitic, biotites very rich in zircon, magnetite, ilmenite and often pseudomorphosed into chlorite, muscovite often resulting from the damouritisation of potassium feldspars or from the leaching of titanium and iron from primary biotites, sillimanite in fine fibroradiated
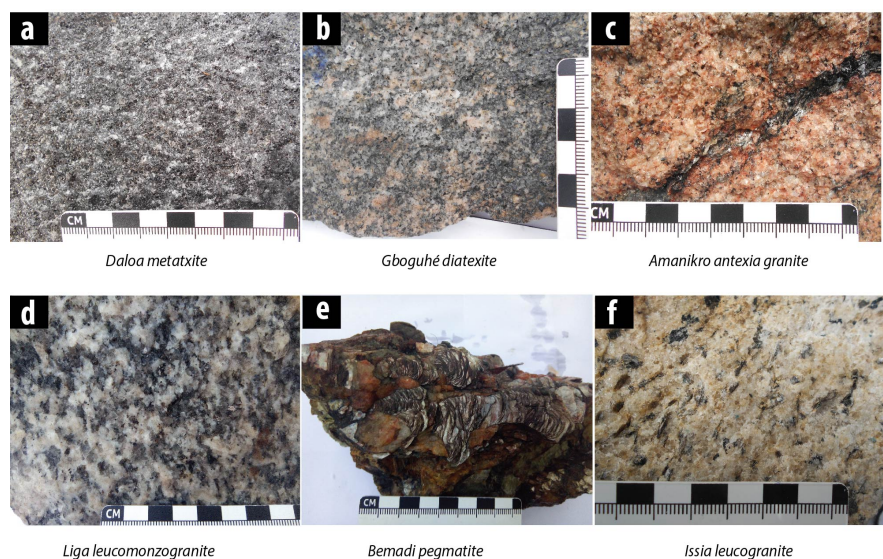

Daloa metatxite *Gboguhé diatexite* *Amanikro antexia granite*

Liga leucomonzogranite *Bemadi pegmatite* *Issia leucogranite*

Figure 3. The Daloa region granitoids.

needles and numerous accessory minerals such as blue apatites, zircon, monazite, xenotime and opaque minerals (ilmenite, rutile, magnetite) according to the cleavages of certain altered biotites.

4.2.2. Granites

The granites cover almost all the rest of the region from the Mimia intrusives in the centre to the town of Issia, with a few flakes of meta-sedimentary rocks. The granites show a mineral paragenesis with two micas very often forming overmicaceous enclaves of orientation concordant with the magmatic fluidity. They are generally two-mica leucogranites or leucomonzogranites (Figures 3(d)-(f)).

The massifs of leucogranites in the study area are made up of megacrysts of quartz and potassium feldspar coarsely intergrown with muscovite and sometimes tourmaline. Biotite is difficult to identify with the naked eye and was only revealed in thin sections because it was often pseudomorphosed into muscovite. The accessory minerals are in order of abundance: apatite, beryl, allanite, xenotime, zircon and opaque minerals (titanomagnetite, ilmenite and rutile).

5. Geochemical Characterization and Interpretation

The chemical composition of the rocks in Daloa can be found in the Appendix attached to the document.

5.1. Geochemical Major Element Composition

The plutonic rocks in this area consist of granite (TM33 and TM44), granodiorite (TM40), tonalite (TM42; TM42_1; TM43).

The granitoids and diorite in the study area show SiO_2 contents between 62.84% and 71.16%, Al_2O_3 between 15.21% and 16.38%, Na_2O between 4.01% and 4.62%; K_2O between 2.09% and 5.17%; CaO between 1.19% and 4.69% and TiO_2 between 0.23% and 0.7%. The loss on ignition (LOI) is far from 1 which shows that these rocks are highly altered.

The analysis of major elements in the Daloa rocks shows that all samples have high SiO_2 (64% - 77%) and high Al_2O_3 (13.7% - 15.9%) contents. In contrast, CaO (0.45% - 4.47%), TiO_2 (0.06% - 0.53%), P_2O_5 (0.06% - 0.57%) and MgO (0.09% - 4.61%) contents are low. The sum of alkalis ($K_2O + Na_2O$) is between 5.01% and 9.21%, which is lower than the values for Al_2O_3, attesting to the very aluminous character of these rocks. The alumina saturation index ($Al_2O_3/(CaO + Na_2O + K_2O)$) of the granitoids ranges from 1.44 to 2.21 indicating that they are hyperaluminous (Dago et al., 2019).

5.2. Characterization, Classification and Nomenclature Based on Major Elements

By analyzing the Shand (1943) diagram modified by Chappell and White (2001), which makes it possible to determine the aluminous character of the rocks, we note that the rocks DAL06 from Daloa, TM42, TM42-1, TM43 of the Tiassalé region are metaluminous and all other rocks are peraluminous (Figure 4). As for
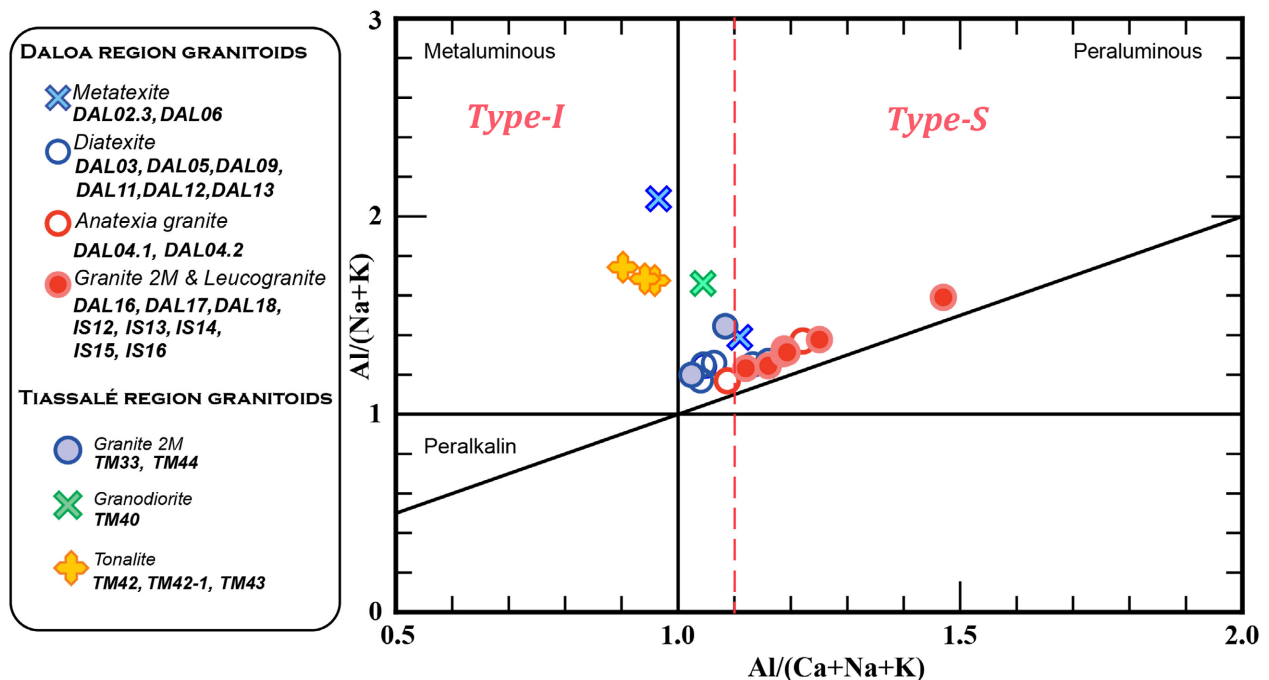
Figure 4. Position of the Daloa and Tiassalé granitoids in the A/CNK vs A/NK diagram of Shand (1943) modified by Chappell and White (2001). The discrimination line (red dashed line) of the granitoids is based on the studies of Maniar and Piccoli (1989).

the origin of the rocks according to the line introduced in this graph by Chappell and White (2001), all rocks in the Tiassalé area are of igneous or infracrustal origin (Granite Type I). In this diagram, the metatexites and diatexites in the Daloa area are of igneous origin; the two-mica granites and leucogranites in the Issia area are of sedimentary or supracrustal origin (Type S granite).

In Middlemost's $Na_2O + K_2O$ (wt %) versus SiO_2 (wt %) diagram (1994), the DAL06 metatexite from Daloa as well as the three tonalite samples from Tiassalé (TM42, TM42-1 and TM43) fall into the tonalite field (**Figure 5**). In this diagram, the Daloa diatexites (DAL11, DAL12, DAL13) and all granitic rocks fall into the granite field. Sample TM40 from Tiassalé and metatexite DAL02.3 from Daloa fall into the granodiorite field. These results confirm the names given to them during the petrographic description. Samples TM33 and TM44 fall into the granite field as do the diatexites, anatexia granites, two-mica granites and leucogranites of the Daloa region.

In Harpum's (1963) K_2O vs Na_2O diagram (**Figure 6**), the two-mica granite sample, the metatexite (DAL02.3) from Daloa and the tonalite-granodiorite samples from Tiassalé fall into the Tonalites-Trondhjemite field. The TM44 granite sample from Tiassalé falls in the granodiorite field as does the DAL06 metatexite and all the diatexites. This position of these migmatites would rather indicate the nature of the protolith from which they were derived than their actual nature. Granite sample TM33 from Tiassalé and all other granitic facies display an adamellite character. The weakly to moderately peraluminous nature of these rocks shows that they were derived from a mantle source with crustal participation.
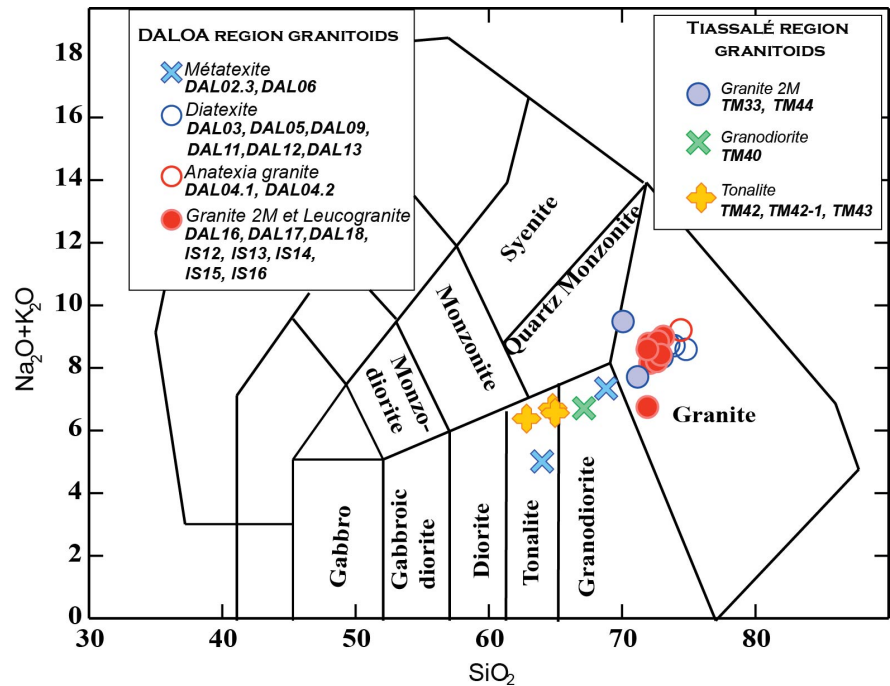
Figure 5. Na₂O + K₂O (wt %) versus SiO₂ (wt %) diagram from Middlemost (1994).
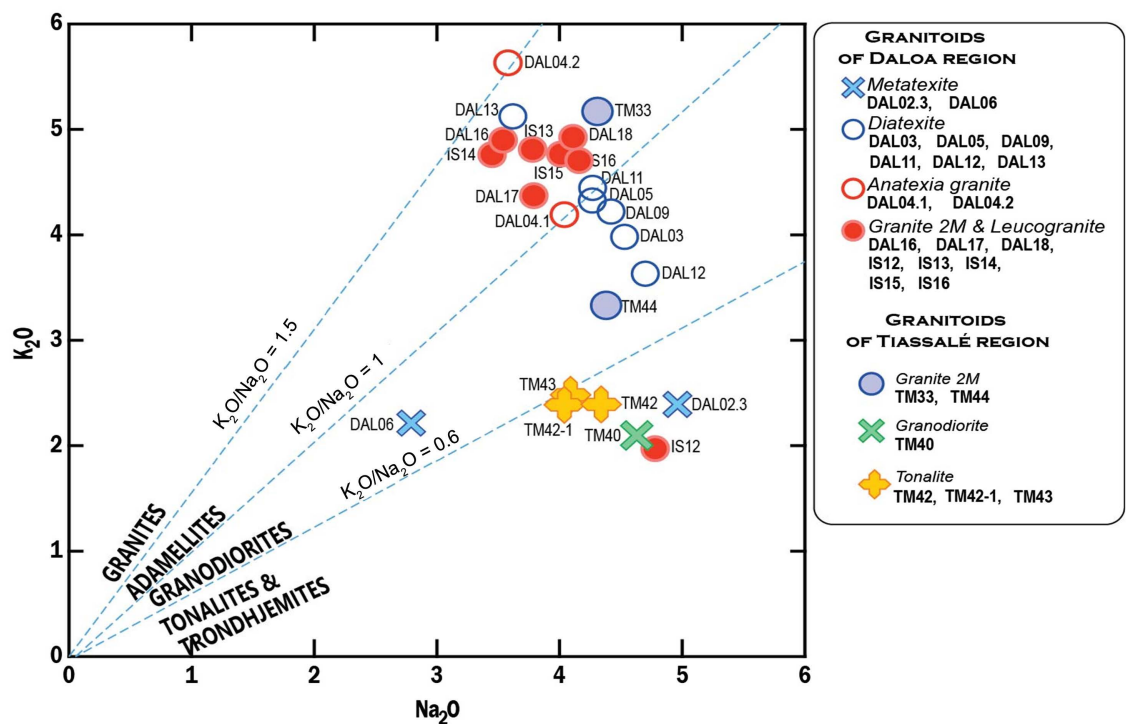
Figure 6. Harpum's (1963) classification and nomenclature diagrams of the granitoids (Na₂O vs K₂O).

5.3. Geochemical Comparison

To understand the geochemical link between the different magmas that generated the intrusive granitoids in the Comoé Basin and those constituting the Ferké batholith, we used Harker diagrams (oxides vs. SiO_2) and multi-element

and rare-earth elements diagrams, as these elements do not fractionate very much in relation to each other.

5.3.1. Harker Diagrams

The Harker elemental plots of Oxides vs SiO_2 show a continuous and linear distribution of representative points of the plutonic rock samples (**Figure 7**). This distribution indicates negative correlations between SiO_2 and the majority of elements, notably Al_2O_3, Fe_2O_3, CaO, TiO_2, MgO, P_2O_5 (**Figure 7**). The proximity of the diatexites to the granitic facies of Daloa suggests a common origin of the rocks in this region.

In the K_2O vs. SiO_2 diagram that allows to determine the magmatic series of the rocks according to Le Bas et al. (1986), all these granitoids show high and medium-K calk-alkaline affinities, except the granite (TM33) and the anatexia granite (DAL04.1), located in the shoshonitic series.

Figure 7. Distribution of granitoids in Harker-type oxide vs SiO_2 diagrams.

The approximately linear distribution of the Daloa diatexites and the Issia granites could indicate the intervention of magmatic mixtures b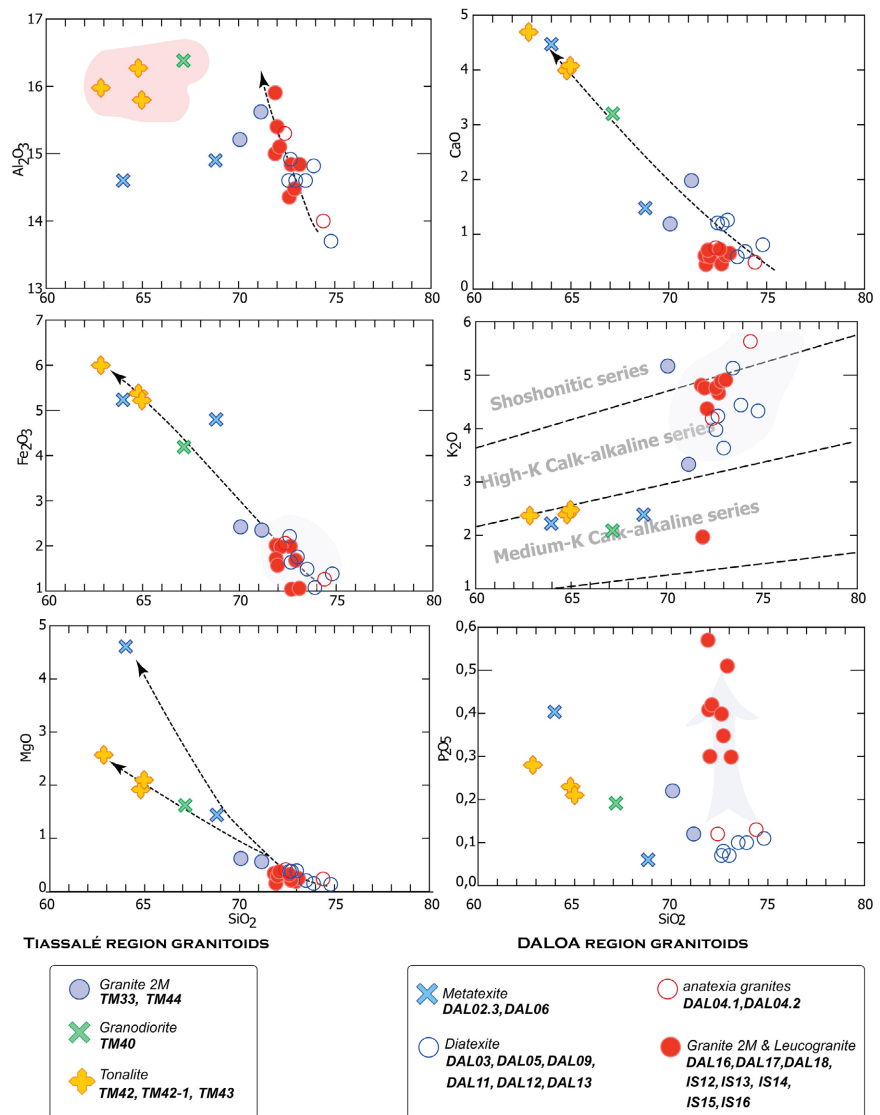etween an acid and a basic magma as well as fractional crystallization processes (Kouchi & Sunagawa, 1985; Liankun & Kuirong, 1989; Zorpi et al., 1989; Orsini et al., 1991; Boukaoud, 2007). In the Tiassalé granitoids, a grouping or regression line is observed that is very different from that of the Daloa granitoids, which probably originated from the same source. Furthermore, the transition elements P_2O_5, TiO_2 and Cr_2O_3 each represent less than 2% in the granitoids and show negative correlations with SiO_2. This is due to the effect of early crystallization processes of rutile, ilmenite and apatite minerals from the beginning of magma formation (Moyen et al., 1997).

Only the metatexite DAL06 (migmatitic granodiorite) has a behavior very close to the granodiorite (TM40) and tonalites (TM42, TM42-1 and TM43) of Tiassalé. As for the Tiassalé granites (TM33 and TM44), they are close in nature to the Daloa granitoids.

The analysis of the behavior of the two families of granitoids in the Haker diagrams (oxides vs. SiO_2) shows that they come from different sources.

5.3.2. Rare Earth Spectra and Multi-Element Diagrams

Overall, the rare earth spectra (Nakamura, 1974) are highly fractionated with an enrichment in LREE and almost no europium (Eu) anomaly. In detail, variations appear between the spectra of each petrographic entity.

The Tiassalé granitoid plutons generally show fairly negatively sloping spectra. The degree of fractionation of the LREEs in relation to the HREEs expressed by the ratio (La/Yb)N varies from 16.10 to 37.90. This fractionation rate appears very important and implies an enrichment in LREE and a significant depletion in HREE, this highliths the importance of the fractionation of accessory minerals incorporating LREE. The spectra of the different plutonites can be superimposed (Figure 8(a)).

The multi-element diagrams of the Comoé plutonic rocks, normalized to the primitive mantle, show strongly negative slopes with an enrichment of lithophilic elements (LILE) and more incompatible elements (Cs, K, Rb, Ba, Th…) compared to elements with high ionic potential (HFSE) and less incompatible elements (Tb, Y, Yb, U, Nb…). In detail, these diagrams are quite comparable and intersect each other (Figure 8(b)).

The K enrichment is thought to be due to the recrystallisation of biotites. The pronounced P and Ti anomalies may be related to the fractionation of apatite, ilmenite and sphene minerals in the melt residue. The negative Nb anomaly suggests crustal contamination of the magma, and is typical of subduction zone magmas.

The rare earth diagrams of the Daloa metatexites and those of the Tiassalé tonalite-granodiorites have similar appearances, although the latter seem to be more enriched in HREE.
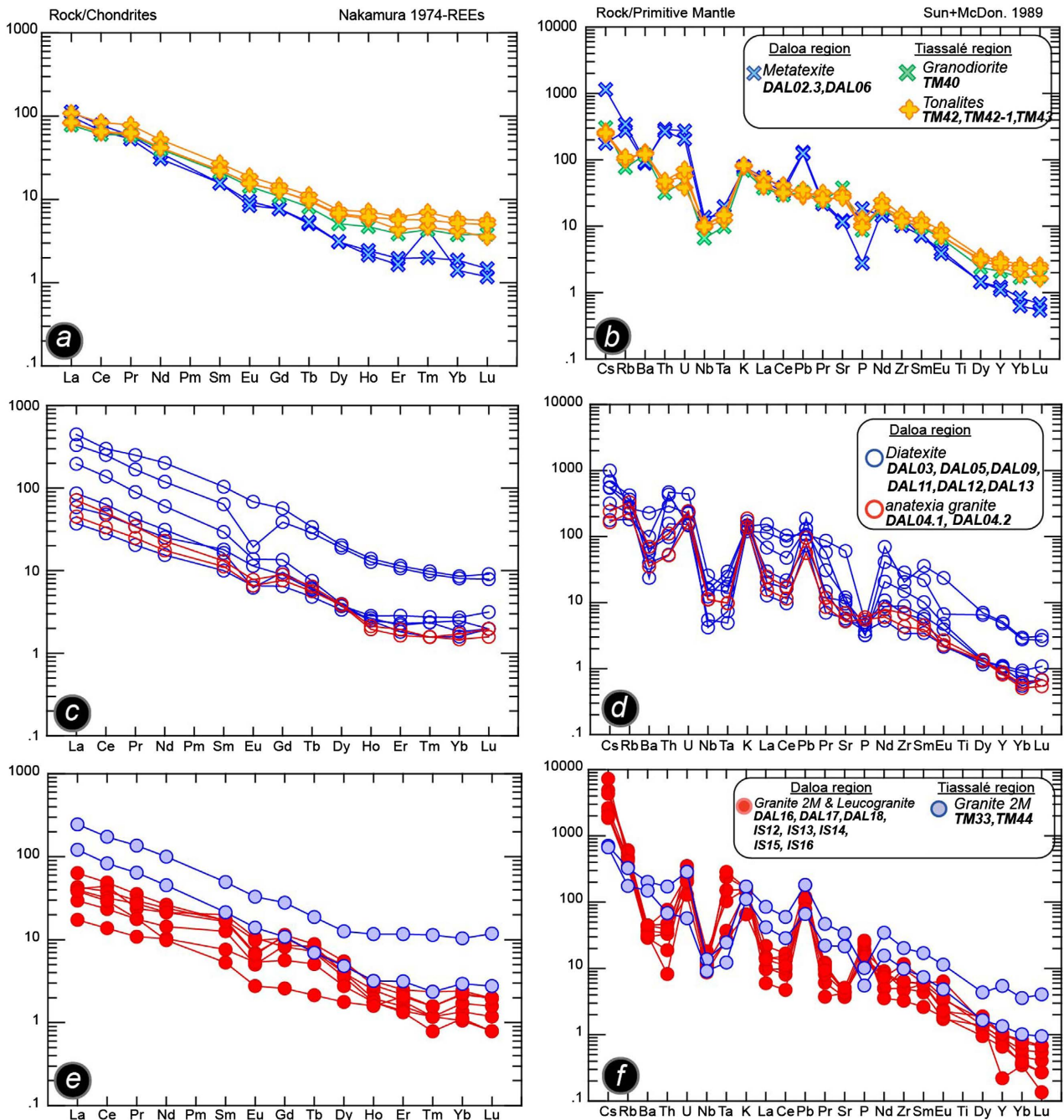
Figure 8. Rare earth spectra (Nakamura, 1974) and multi-element diagrams (Sun & McDonough, 1989).

In the multi-element diagram, some small differences are to be noted. The Cs content of the metatexites can reach up to 1000 times the value of the primitive mantle; the value of Th and U in the metatexites can be three times that of the tonalite-granodiorites of Tiassalé. There is a positive anomaly in Pb and a negative anomaly in P which can be explained by the apatite richness of these rocks.

For the Daloa diatexites and anatexia granites, the graphs show the same pattern, suggesting that they were differentiated from the same source (**Figure 8(c)** and **Figure 8(d)**).

A comparative study of the diagrams of the granites of the Tiassalé region shows that they are richer in rare earths elements and very flattened compared to the granites of the Daloa region (Figure 8(e)) where the Eu anomaly is more marked.

In the multi-element diagram, the difference between these two granite groups is clearer (Figure 8(f)). The Daloa granites show a Cs enrichment that varies from 2000 to 8000 times and the Tiassalé granites between 700 and 800 times the Cs value in the primitive mantle. A positive P anomaly is observed in the Daloa granites, unlike the Tiassalé granites, which show a negative anomaly in this element. A very high Ta value is also observed in the Daloa granites (between 100 and 300 times) compared to the Tiassalé granites which have a Ta content between 10 and 20 times the Ta value of the primitive mantle.

6. Geodynamic Context of the Setting up of the Plutons

In order to identify the geodynamic setting of the rocks of the Comoé basin (Tiassalé region) and those of the Ferké batholith (Daloa region), the geochemical data were projected into the Rb versus Y + Nb binary diagram of Pearce et al. (1984). This diagram provides information on the petrogenetic and geotectonic relationships of the granitoids (Figure 9).

Due to their low Ta, Y and Nb contents, all Tiassalé rocks, migmatites and anatexia granites from the Daloa area fall into the field of volcanic arc granites (VAG) and are therefore of infracrustal origin (Figure 9(b)). Except for sample IS12 which has a trondjhemite character (see Harpum diagram, Figure 6) which also falls in the VAG field, the leucogranites and two-mica granites from the Daloa area all fall in the Syn-COLG field and are therefore of supracrustal origin.

7. Discussion

7.1. Petrological Characteristics

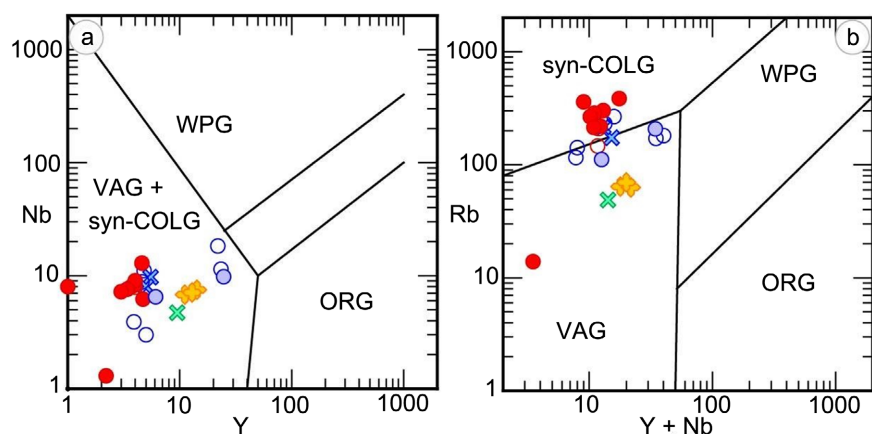The plutons of the Tiassalé zone show chemical compositions almost similar to

Figure 9. Tectonic context discrimination diagram for Rb granitoids as a function of Y + Nb after Pearce et al. (1984).

those of other birimic domains; in particular those of the Singrobo and Dabakala groups, respectively studied by Teha (2019) and by Gasquet et al. (2003) and Gnanzou (2014). Most indicate medium calc-alkaline compositions, but some tend towards the alkaline pole (shoshonite series). The calc-alkaline affinity of the latter would come from spatial association with the metasedimentary rocks of the Comoé basin (Glodji, 2012).

Granodiorites and tonalites are metaluminous and granites are moderately peraluminous and all correspond to Type I granites of Pitcher's (1983) classification.

Based on their intrusive mode, petrographic and chemical characteristics (low K/Na ratios), as well as the position of the Tiassalé granitoids in the classification diagram of Chappell and White (1974) and the Rb vs Y + Nb diagram of Pearce et al. (1984), it can be stated that the Tiassalé plutonites as a whole are derived from an igneous source. In the rare earth diagrams and multi-element diagrams, the graphs of these rocks overlap exactly, confirming their common origin.

As for the rocks of the Daloa region, they show a continuous sequence from metatexites to leucogranites, which suggests that the rocks of this region are derived from the same source magma37 that underwent several cycles. Originally, the TTG rocks underwent partial melting to produce the metatexites and then the diatexites. The sediments resulting from the meteoric alteration of the TTG would have been transformed by simple metasomatosis into leucogranite thanks to the heat brought by the late intrusives with two micas from Mimia.

The rocks of the Daloa region are clearly distinct from one another, which would imply, from a geochemical point of view, the intervention of processes such as differentiation and/or contamination of the magmas that generated these rocks. One thing is certain: these rocks have a common origin (see Harker diagram, Figure 8; multi-element diagrams, Figure 9).

The presence of diorite intrusions associated with granitoid intrusions in the Tiassalé region (Téha et al., 2018), suggests the involvement of a mantle source (Bussy, 1990; Abdallah, 2008). Ouattara and Koffi (2014) and Téha et al. (2018) propose a double origin (anatexic and mantle) in the genesis of these granitoids. As for the metatexites and diatexites of Daloa which are migmatites thus suggesting anatexia and their belonging to the type I granites group (see Figure 4), one can also grant them a double origin (mantle and then anatectic). This is corroborated by the work of Chappell and White (1974) who attribute the origin of type I or igneous granites on the one hand to the melting of the mantle and on the other hand to the melting of crystalline rocks of the continental crust. Their metaluminous character is, according to Debon and Lefort (1983), due to a mantle origin, or at least to a source derived from the mantle. As for the two-mica granites and leucogranites, they are peraluminous plutons that are linked to the continental crust.

These flat rare earth spectra with a slight slope are characteristic of Archean GTTs (Martin & Moyen, 2011). The highly fractionated spectra; the near-zero Eu anomaly (Eu/Eu*) and the negative Nb, Ti anomalies give the tonalite-

granodiorites of Tiassalé and the migmatites of Daloa the characteristics of Archean GTTs (Dago, 2020). For Martin (1999), the absence of Eu anomaly would result from the melting of a subducted oceanic crust, hydrated in a moderately deep subduction zone, which reacted with the mantle wedge at the base of the adjacent continental crust. Furthermore, the Nb anomaly also observed on the multi-element diagrams are according to Dupuis (2005) and Hoffer (2008) confirm the existence of subduction which would have generated these magmas. On the other hand, the significant negative Nb anomalies indicate the role played by titaniferous and/or amphibole phases (Martin, 1999). The negative Eu anomaly found in some leucogranite graphs would indicate plagioclase fractionation. These granites are highly enriched in LILE and show spectra marked by negative anomalies in Nb, Sr and Ti, characteristic of calc-alkaline magmas from orogenic zones and continental crust. The arachnograms of these rocks are highly fractionated with a weak or even absent europium anomaly (Eu/Eu*), low Ni and Cr contents and a K_2O/Na_2O ratio of less than 0.5, giving them the characteristics of potassic GTTs. These characteristics make it possible to link their emplacement to a subduction context. Plutonic rocks are associated with volcanic and syn-collisional arc granites, which were emplaced in a subduction environment (Dago, 2020).

7.2. Source of Magmas

The comparative study of these intrusive granites in the Comoé basin (Tiassalé granitoids) and the granites forming the Ferké batholith (Daloa granitoids) shows some similarities in that they are close to the TTG. But all the analyses show that they are quite different. Eu anomaly almost non-existent in Tiassalé granites unlike Daloa granites. The Tiassalé granitoids are more enriched in rare earths elements than the Daloa granitoids (Figure 8). The Tiassalé granitoids are of infracrustal origin (Type I), whereas the Daloa granitoids, although having a primitive infracrustal source, have undergone a polycyclic evolution until they produce granites in supracrustal conditions. This is evidenced by the fact that these granitoids align with common regression curves (see Harker diagram, Figure 7).

8. Conclusion

The comparative study of the granitoids of the Comoé basin and those of the Daloa region has shown that the West African Paleoproterozoic basement is the result of various magmatic activities generating rocks of very diverse nature.

The granitoids emplaced in the Comoé basin are derived from the direct crystallisation of mantle magmas. These granitoids are often intrusive and dome-shaped within the volcano-sedimentary and meta-sedimentary rocks of the Comoé basin, reflecting syntectonic emplacement; they correspond to Type I granites. The granitoids of the Daloa region constitute a magmatic suite evolving from migmatitic facies (metatexites, diatexites and anatexia granites) to leucogranites. The migmatites were emplaced in a volcanic arc context (Type I) and the s.s. granites

in a syn-collisional context. (Type S). Three interlocking origins are thus denoted to produce a diverse range of rocks in the Daloa region: magmatic, anatectic and/or metasomatic. The granitoids of the Comoé basins are quite different from those of the Ferkessedougou batholith.

Conflicts of Interest

The authors declare no conflicts of interest regarding the publication of this paper.

References

Abdallah, N. (2008). *Geochemistry and Geochronology of the Pan-African Magmatic Intrusions of the Aegean-Aleksod Terrane: Example of the Granitic Massifs of Ounane, Tihoudaine and Tisselliline (Central Hoggar, Algeria)* (202 p). Thesis Doc, University of Science and Technology Houari Boumediene.

Abouchami, W., Boher, M., Michard, A., Albarede, F., & Major, A. (1990). 2.1-Ga Event of Mafic Magmatism in West Africa: An Early Stage of Crustal Accretion. *Journal of Geophysical Research: Solid Earth, 95,* 17605-17629.
https://doi.org/10.1029/JB095iB11p17605

Alric, G. (1985). Contribution à l'étude pétrographique des roches magmatiques non granitoïdiques birrimiennes de la Haute-Comoé (N-E Côte d'Ivoire). *Annales de l'Université d'Abidjan. Série C, Sciences. Université d'Abidjan, tome XXI, tome XXI.*

Alric, G., Gibert, P., & Vidal, M. (1987). Le problème des grauwackes birimiennes de Côte d'Ivoire: Une revue et des données nouvelles. Le cas de l'unité de la Comoé. *Comptes rendus de l'Académie des Sciences, 304,* 289-294.

Arnould, A. (1961). *Etude géologique des migmatites et granites précambriens du Nord de la Côte d'Ivoire et de la Haute-Volta méridionale* (174 p). Bureau de Recherches Géologiques et Minières (BRGM).

Billa M., Feybesse J.-L., Bronner G., Lerouge C., Milesi J.-P., Traore, S., & Diaby, S. (1999). Les formations à quartzites rubanés ferrugineux des monts Nimba et du Simandou: Des unités empilées tectoniquement, sur un soubassement plutonique archéen (craton de kénéma-man), lors de l'orogène éburnéen. *Comptes Rendus de l'Académie des Sciences- Series IIA-Earth and Planetary Science, 329,* 287-294.
https://doi.org/10.1016/S1251-8050(99)80248-1

Boher, M. (1991). *Croissance crustale en Afrique de l'Ouest à 2,1 Ga. Apport de la géochimie isotopique* (180 p). Doctorat, Université Henri Poincaré - Nancy 1.

Bonhomme, M. (1962). *Contribution à l'étude géochronologique de la plate-forme de l'Ouest africain* (62 p). Annales de la Faculté des Sciences No. 5, Université Clermont Auvergne.

Boukaoud, E. H. (2007). *Étude pétrographique et géochimique des pegmatites de Sidi Mezghiche (Wilaya de Skikda, nord-est algérien)* (134 p). Master's Thesis, Université des Frères Mentouri Constantine 1.

Bussy, F. (1990). *Petrogenesis of Micrograined Enclaves Associated with Calc-Alkaline Granitoids: Example of the Variscan Massifs of Mont Blanc (Western Alps) and Miocene Monte Capanne (Isle of Elba, Italy)* (356 p). Thesis, University of Lausanne.

Casanova, R. (1973). *Geochemistry and Mineralogy of the Eburnian Granitoids of the Ivory Coast* (327 p). Thèse de Doctorat d'Etatès sciences, Université de Nice.

Chappell, B. W., & White, A. J. R. (1974). Two Contrasting Granite Types. *Pacific Geology, 8,* 173-174.

Chappell, B. W., & White, J. R. (2001). Two Contrasting Granite Types: 25 Years Later. *Australian Journal of Earth Sciences, 48,* 489-499. https://doi.org/10.1046/j.1440-0952.2001.00882.x

Dago, A. G. B. (2020). *Les granitoïdes birimiens de la région de Daloa (centre-ouest de la Côte d'Ivoire): Genèse et implication dans l'évolution thermique du craton ouest africain* (221p). Thesis doc. ès Sciences Univ. FHB Abidjan.

Dago, A. G. B., Coulibaly, Y., & Ouattara, Z. (2019). Petrographic and Geochemical Typology of the Granitoids of the Daloa Region in West-Central Côte d'Ivoire. *Afrique SCIENCE, 15,* 208-221.

Debon, F., & Lefort, P. (1983). A Chemical-Mineralogical Classification of Common Plutonic Rocks and Associations. *Transactions of the Royal Society of Edinburgh, Earth Sciences, 73,* 135-149. https://doi.org/10.1017/S0263593300010117

Doumbia, S. (1997). *Geochemistry, Geochronology and Structural Geology of the Birimian Formations of the Katiola-Marabadiassa Region (Centre-North of Ivory Coast): Magmatic Evolution and Geodynamic Context of the Paleoproterozoic* (253 p). Thèse de Doctorat, Université d'Orléans.

Dupuis, C. (2005). *Petrology and Geochemistry of the Mesozoic Tethyan Provinces Related to the Yarlung-Zangbo Suture Zone, Tibet* (268 p). Ph.D. Thesis, Laval University.

Feybesse, J.-L., Billa, M., Guerrot, C., Duguey, E., Lescuyer, J.-L., Milesi, .-P., & Bouchot, V. (2006). The Paleoproterozoic Ghanaian Province: Geodynamic Model and Ore Controls, Including Regional Stress Modeling. *Precambrian Research, 149,* 149-196. https://doi.org/10.1016/j.precamres.2006.06.003

Gasquet, D., Barbey, P., Adou, M., & Paquette, J. L. N. (2003). Structure Sr-Nd Isotope Geochemistry and Zircon U-Pb Geochronology of the Granitoids of the Dabakala Area (Côte d'Ivoire): Evidence for a 2.3 Ga Crustal Growth Event in the Palaeoproterozoic of West Africa? *Precambrian Research, 127,* 329-354. https://doi.org/10.1016/S0301-9268(03)00209-2

Glodji, A. L. (2012). *The Kandi Shear Zone and Associated Magmatism in the Savalou-Dassa Region (Benin): Structural, Petrological and Geochronological Study* (277 p). PhD Thesis, University of Jean Monnet Saint-Etienne et d'Abomey-Calavi.

Gnanzou, A. (2014). *Study of the Volcano-Sedimentary Series of the Dabakala Region (North-East Ivory Coast): Genesis and Magmatic Evolution* (303 p). Contribution to the Knowledge of the Bobosso Gold Mineralisation in the Haute-Comoé Series, PhD Thesis, Université Paris-Saclay, and Université Félix-Houphouët-Boigny.

Harpum, J. R. (1963). Petrographic Classification of Granitic Rocks by Partial Chemical Analysis. *Tanganyika Geological Survey, 10,* 80-88.

Hirdes, W., & Davis, D. W. (1998). First U-Pb Zircon Age Extrusive Volcanism in the Birimian Supergroup of Ghana, West Africa. *Journal of African Earth Sciences, 27,* 291-294. https://doi.org/10.1016/S0899-5362(98)00062-1

Hirdes, W., Davis, D. W., Lüdtke, G., & Konan, G. (1996). Two Generations of Birimian (Paleoproterozoic) Volcanic Belts in Northeastern Côte d'Ivoire (West Africa): Consequences for the 'Birimian Contoversy'. *Precambrian Research, 80,* 173-191. https://doi.org/10.1016/S0301-9268(96)00011-3

Hoffer, G. (2008). *Partial Melting of a Metasomatised Mantle by an Adakitic Liquid: Geochemical and Experimental Approaches to the Genesis and Evolution of Magmas in the Ecuadorian Back-Arc* (335 p). PhD Thesis, Blaise Pascal University.

Jessell, M. W., Amponsah, P. O., Baratoux, L., Asiedu, D. K., Loh, G. K., & Ganne, J. (2012).

Crustal-Scale Transcurrent Shearing in the Paleoproterozoic Sefwi-Sunyani-Comoé Region, West Africa. *Precambrian Research, 212,* 155-168. https://doi.org/10.1016/j.precamres.2012.04.015

Kouchi, A., & Sunagawa, I. (1985). A Model for Mixing Basaltic and Dacitic Magmas as Deduced from Experimental Data. *Contributions to Mineralogy and Petrology, 89,* 17-23. https://doi.org/10.1007/BF01177586

Le Bas, M. J., Le Maitre, R. W., Streckeisen, A., & Zanettin, B. (1986). A Chemical Classification of Volcanic Rocks Based on the Total Alkali-Silica Diagram. *Journal of Petrology, 27,* 745-750. https://doi.org/10.1093/petrology/27.3.745

Liankun, S., & Kuirong, Y. (1989). A Two-Stage Crust-Mantel Interaction Model for Mafic Microgranular Enclaves in the Daning Granodiorite Pluton, Guangxi, China. In J. Didier, & B. Barbarin (Eds.), *Enclaves and Granite Petrology* (Developments in Petrology, Vol. 13, pp. 95-110). Elsevier.

Lompo, M. (2010). Structural Evolution of Paleoproterozoïc Belts (Eburnean Event) in the Man- Leo Shield, West African Craton. Key Structures for Vertical to Transcurrent Tectonics. *Journal of African Earth Sciences, 58,* 19-36. https://doi.org/10.1016/j.jafrearsci.2010.01.005

Maniar, P. D., & Piccoli, P. M. (1989). Tectonic Discrimination of Granitoids. *GSA Bulletin, 101,* 635-643. https://doi.org/10.1130/0016-7606(1989)101%3C0635:TDOG%3E2.3.CO;2

Martin, H. (1999). Adakitic Magmas: Modern Analogues of Archean Granitoids. *Lithos, 46,* 411-429. https://doi.org/10.1016/S0024-4937(98)00076-0

Martin, H., & Moyen, J. F. (2011). Trondhjemite-Tonalite-Granodiorite Suites and Archean Sanukitoids. *Geochronique, 120,* 31-38.

Middlemost, E. A. K. (1994). Naming Materials in the Magma/Igneous Rock System. *Earth-Science Reviews, 37,* 215-224. https://doi.org/10.1016/0012-8252(94)90029-9

Milesi, J. P., Feybesse, J. L., Pinna, P., Deschamps, Y., Kampunzu, H., Muhongo, S. et al. (2004). Geological Map of Africa 1:10000000. "SIGAfrique Project". In *20th Conference of African Geology.* Bureau de Recherches Géologiques et Minières (BRGM).

Milési, J.-P., Ledru, P., Feybesse, J.-L., Dommanget, A., & Marcoux, E. (1992). Early Proterozoic Ore Deposits and Tectonics of the Birimian Orogenic Belt, West Africa. *Precambrian Research, 58,* 305-344. https://doi.org/10.1016/0301-9268(92)90123-6

Moyen, J. -F., Martin, H., & Jayananda, M. (1997). Origin of the Closepet Finite-Archaean Granite (South India): Contributions of Geochemical Modelling of Trace Element Behaviour. *Comptes rendus de l'Académie des Sciences, 325,* 659-664.

Nakamura, N. (1974). Determination of REE, Ba, Fe, Mg, Na and K in Carbonaceous and Ordinary Chondrites. *Geochimica et Cosmochimica Acta, 38,* 757-775. https://doi.org/10.1016/0016-7037(74)90149-5

Orsini, J. B., Cocirta, C., & Zorpi, M. J. (1991). Genesis of Mafic Microgranular Enclaves Trough Differenciation of Basic Magmas, Mingling and Chemical Exchanges with Their Host Granitoid Magmas. In J. Didier, & B. Barbarin (Eds.), *Enclaves and Granite Petrology* (Developments in Petrology, Vol. 13, pp. 445-463). Elsevier.

Ouattara, G. (1998). *Structure du batholite de Ferkéssédougou (secteur de Zuenoula, Côte d'Ivoire): Implications sur l'interprétation de la géodynamique du paléoproterozoïque d'Afrique de l'ouest a 2.1 Ga* (344 p). Thesis, Université d'Orléans.

Ouattara, G., & Koffi, G. B. (2014). Typologie des granitoïdes de la région de Tiassalé (Sud de la Côte d'Ivoire - Afrique de l'Ouest): Structurologie et Relations Génétiques. *Afrique SCIENCE, 10,* 258-276.

Pearce, J. A., Harris, N. B. W., & Tindle, A. G. (1984). Trace Element Discrimination Diagrams for the Tectonic Interpretation of Granitic Rocks. *Journal of Petrology, 25,* 956-953. https://doi.org/10.1093/petrology/25.4.956

Pitcher, W.S. (1983). Granite Type and Tectonic Environment. In K. Hsu (Ed.), *Mountain Building Processes* (pp 19-40). Academic Press.

Pouclet, A., Doumbia, S., & Vidal, M. (2006). Geodynamic Setting of the Birimian Volcanism in Central Ivory Coast (Western Africa) and Its Place in the Palaeoproterozoic Evolution of the Man Shield. *Bulletin de la Société Géologique de France, 177,* 105-121. https://doi.org/10.2113/gssgfbull.177.2.105

Pouclet, A., Vidal, M., Delor, C., Simeon, I., & Alric, G. (1996). Le volcanisme birimien du nord-est de la Côte d'Ivoire, mise en évidence de deux phases volcano-tectoniques distinctes dans l'évolution géodynamique du Paléoprotérozoïque. *Bulletin Société Géologique de France, 3,* 307-319.

Shand, S. J. (1943). *Eruptive Rocks. Their Genesis, Composition, Classification, and Their Relation to Ore Deposits with a Chapter on Meteorite.* John Wiley & Sons.

Sun, S. S., & McDonough, W. F. (1989). Chemical and Isotopic Systematics of Oceanic Basalts and Implications for Mantle Composition and Processes. *Geological Society, London, Special Publications, 42,* 313-345.

Tagini, B. (1971). *Structural Outline of the Ivory Coast. Essai de géotectonique régionale* (266 p). Thèse de Doctorat, Université de Lausanne.

Taylor, P. N., Moorbath, S., Leube, A., & Hirdes, W. (1992). Early Proterozoic Crustal Evolution in the Birimian of Ghana: Constraints from Geochronology and Isotope Geochemistry. *Precambrian Research, 56,* 97-111. https://doi.org/10.1016/0301-9268(92)90086-4

Teha, K. R. (2019). *The Eburnian Formations of the Southwest Comoé Basin and the Singrobo Area (Southern Ivory Coast): Petrology, Structural Analysis and Associated Magmatism* (218 p). PhD Thesis, Université Félix-Houphouët-Boign.

Téha, K. R., Kouamelan, A. N., Allialy, M. E., Djro, S. C., Houssou, N. N., Koffi, Y. A. et al. (2018). Petrographic and Geochemical Characters of Birimian Granitoids from the Comoé Basin and Surroundings (Southern Ivory Coast). *International Journal of Engineering Science Invention, 7,* 16-25.

Vidal, M., Gumiaux, C., Cagnard, F., Pouclet, A., Ouattara, G., & Pichon, M. (2009). Evolution of a Paleoproterozoic "Weak Type" Orogeny in the West African Craton (Ivory Coast). *Tectonophysics, 477,* 145-159. https://doi.org/10.1016/j.tecto.2009.02.010

Zorpi, M. J., Coulon, C., Orsini, J. B., & Cocirta, C. (1989). Magma Mingling, Zoning and Emplacement in Calc-Alkaline Granitoid Plutons. *Tectonophysics, 157,* 315-329. https://doi.org/10.1016/0040-1951(89)90147-9

Appendix

Table A1. Composition of major elements (%wt) and trace elements (ppm).

Sample	UTM Zone	Easting (X)	Northing (Y)	SiO₂	Al₂O₃	Fe₂O₃	z CaO	MgO	Na₂O	K₂O	MnO	TiO₂	P₂O₅	Cr₂O₃	Ba	Be	Co	Cs	Ga	Hf	Nb	Rb
DAL02.3	29N	789,745	766,731	68.8	14.9	4.8	1.48	1.44	4.96	2.38	0.04	0.53	0.06	0.01	165	2	8.1	4.3	27.5	8	18.3	181
DAL06	29N	783,206	755,175	64	14.6	5.24	4.47	4.61	2.79	2.22	0.09	0.48	0.4	0.04	1586	4	18.5	7.9	16.6	6.1	11.4	170.9
DAL05	29N	783,401	755,636	74.8	13.7	1.38	0.81	0.13	4.26	4.33	0.02	0.06	0.11	0.01	453	2	1.1	2.5	17.8	3.6	3	141.5
DAL12	29N	766,352	747,149	73	14.6	1.75	1.26	0.39	4.71	3.63	0.03	0.22	0.07	0.01	617	2	2.4	1.4	20.3	4.4	9.7	173.3
DAL03	29N	794,908	774,497	72.6	14.6	2.21	1.2	0.38	4.53	3.98	0.03	0.22	0.07	0.01	693	3	2.4	1.4	17.4	4.7	3.9	115.7
DAL04.1	29N	795,755	769,145	72.4	15.3	2.01	0.75	0.41	4.03	4.19	0.02	0.13	0.12	0.01	246	2	1.8	1.3	21.6	1.7	8	146.2
DAL04.2	29N	796,174	769,182	74.4	14	1.26	0.49	0.23	3.58	5.63	0.02	0.09	0.13	0.01	489	1	1.2	1.9	15.4	2.6	7.9	208.8
DAL09	29N	780,476	740,720	72.7	14.9	1.64	1.19	0.37	4.42	4.22	0.02	0.19	0.08	0.01	655	6	1.9	9	20.3	3.4	8	216.8
DAL11	29N	781,038	749,710	73.9	14.8	1.06	0.68	0.15	4.27	4.44	0.03	0.08	0.1	0.01	279	5	0.6	4.4	20.6	1.5	8.8	231.2
DAL13	29N	754,001	739,440	73.5	14.6	1.47	0.59	0.21	3.62	5.13	0.02	0.12	0.1	0.01	399	5	0.9	5.4	21.9	2.4	11.1	266.5
DAL17	29N	767,600	717,242	72.1	15.1	1.97	0.61	0.33	3.79	4.37	0.02	0.14	0.42	0.01	202	4	1.1	18.4	16.6	1.8	8.3	219.2
DAL18	29N	781,013	719,170	71.9	15.1	1.8	0.7	0.36	3.91	4.67	0.03	0.23	0.4	0.01	301	7	1.6	12.3	20.3	3.4	5.6	390.7
IS15	29N	772,939	731,650	72	15.4	1.6	0.66	0.31	4.01	4.76	0.02	0.16	0.3	0.01	296	2	1	16.8	19.3	1.7	6.8	246.1
IS16	29N	757,092	723,302	72.7	14.84	1.04	0.48	0.22	4.16	4.69	0.01	0.11	0.35	0.01	206.8	8	31.5	34.2	22.4	1.7	8	359.6
IS18	29N	763,268	720,342	71.9	15.1	1.8	0.7	0.36	3.91	4.67	0.03	0.23	0.4	0.01	301	7	1.6	12.3	20.3	3.4	5.6	390.7
IS 14	29N	767,444	720,492	72.6	14.4	1.94	0.71	0.34	3.45	4.76	0.02	0.15	0.4	0.01	312	5	1.2	15.8	17.2	2.1	6.2	213.8
DAL16	29N	779,689	719,555	72.9	14.5	1.68	0.61	0.21	3.54	4.88	0.03	0.07	0.51	0.01	223	22	0.8	57.1	15.8	1.7	7.2	265.9
IS12	29N	765,848	717,278	71.9	15.9	2	0.45	0.19	4.78	1.97	0.06	0.09	0.57	0.01	301	5	1.1	38.6	27.3	2.1	12.9	385.5
IS13	29N	759,662	724,386	71.9	15	1.72	0.63	0.34	3.78	4.81	0.02	0.17	0.41	0.01	258	7	1.5	20.7	18.8	2.2	7.6	286.1
TM33	30N	299,136	649,553	70.07	15.21	2.42	1.19	0.62	4.31	5.17	0.03	0.39	0.22	0.01	1411	4	4	5.6	20.6	5.8	9.8	207.5
TM40	30N	295,906	656,995	67.14	16.38	4.19	3.2	1.62	4.62	2.09	0.06	0.48	0.19	0.01	826	1	10	2.4	18.1	3.5	4.7	48.7
TM42	30N	297,131	660,902	64.79	16.27	5.39	3.99	1.92	4.33	2.39	0.08	0.67	0.23	0.01	898	1	14.7	1.9	17.4	4.1	6.8	64.1
TM42-1	30N	297,131	660,902	62.84	15.97	6	4.69	2.57	4.01	2.37	0.09	0.7	0.28	0.01	897	4	17.3	2.1	16.6	4.4	7.5	63
TM43	30N	314,902	651,642	64.97	15.8	5.22	4.07	2.1	4.06	2.5	0.08	0.59	0.21	0.01	846	2	15.1	2	17.5	3.7	7.1	69.7
TM44	30N	295,734	657,095	71.16	15.62	2.35	1.98	0.56	4.38	3.33	0.04	0.23	0.12	0.01	1041	1	3.5	5.3	18	3.3	6.5	111.1

Sample	Sr	Your	Th	U	V	W	Zr	Y	The	This	Pr	Nd	Sm	Eu	Gd	Tb	Dy	Ho	Er	Tm	Yb	Lu	Mo	Cu	Pb	Zn
DAL02.3	204.1	0.7	39.8	9.3	32	0.5	319.3	21.9	78.6	153.8	15.93	55.6	9.74	1.12	7.95	1.07	4.79	0.72	1.76	0.23	1.37	0.2	0.2	3.4	9.2	125
DAL06	1272	0.6	24.6	4.7	78	0.5	228.3	23.4	105.7	183.3	23.82	94.2	15.87	3.96	11.65	1.26	5.15	0.79	1.89	0.25	1.45	0.23	0.2	1.7	7.6	57
DAL05	223.2	0.3	8.3	5	18	0.5	99.7	5	13.9	29.1	3.26	11.8	2.75	0.66	1.83	0.22	0.96	0.16	0.47	0.07	0.46	0.08	0.1	1.6	13.2	12
DAL12	254.6	0.6	24.5	5.7	18	0.5	147	5.5	37	67.8	6.53	22.7	3.19	0.73	2.12	0.24	1.06	0.17	0.44	0.06	0.41	0.05	0.1	2.8	9.2	38
DAL03	251.7	0.2	36.7	3.1	15	0.5	166.3	3.9	46.6	84.4	8.49	28.1	4.49	0.8	2.78	0.28	1	0.14	0.3	0.04	0.27	0.05	0.2	6.8	9.3	33

Continued

DAL04.1	109.8	0.4	4.4	3.4	9	0.5	48.5	3.7	10.7	20.4	2.36	8.2	1.72	0.38	1.57	0.21	0.97	0.11	0.27	0.04	0.25	0.04	0.2	7.3	4	33
DAL04.2	145.7	0.4	9.4	5.1	8	0.5	76.7	4	16.9	30.7	3.25	10.7	2	0.45	1.84	0.24	0.99	0.12	0.32	0.04	0.29	0.05	0.2	1.6	6.8	22
DAL09	242.1	0.8	22.6	4.3	14	0.5	114.1	5	32.8	57.7	5.97	19.4	3.2	0.65	2.14	0.25	1.07	0.15	0.37	0.13	0.31	0.04	0.1	15.7	8.8	40
DAL11	120.8	1	4.5	4.8	8	0.5	37.9	4.6	8.8	17.3	1.94	7.2	1.53	0.38	1.33	0.18	0.85	0.15	0.36	0.06	0.42	0.05	0.1	1.2	5.2	20
DAL13	112.9	1.2	13.3	3.2	12	0.6	75.2	4.8	20.4	38.7	4.06	14.6	2.5	0.36	1.96	0.23	0.94	0.14	0.38	0.06	0.31	0.05	0.2	12.2	5.2	17
DAL17	78.2	1.5	1.6	6.3	10	1.1	56.4	4	7	14.3	1.68	6.7	1.93	0.29	1.76	0.31	1.01	0.14	0.3	0.03	0.23	0.03	0.2	3.7	7.2	34
DAL18	79.4	0.6	11.4	8	20	0.5	109.3	3	20.2	45.4	5.92	23.5	5	0.44	2.83	0.29	0.89	0.11	0.24	0.03	0.25	0.04	0.9	3.9	4.9	59
IS15	91.6	1	2.8	3.5	13	0.7	57.1	3.5	9.7	18.9	2.25	9.1	2.12	0.33	1.68	0.22	1.01	0.14	0.26	0.03	0.26	0.04	0.1	3.2	5	36
IS16	95.4	6.14	2.83	7.4	12	1.2	109.6	1	6.67	17.47	3.2	6.83	2.67	1.07	2.15	0.47	1.12	0.12	0.37	0.05	0.17	0.01	0.2	2.2	8.49	5.3
IS18	79.4	0.6	11.4	8	20	0.5	109.3	3	20.2	45.4	5.92	23.5	5	0.44	2.83	0.29	0.89	0.11	0.24	0.03	0.25	0.04	0.9	3.9	4.9	59
IS 14	107.6	1.1	3.3	2.7	10	0.5	71.2	4.7	9.4	19.5	2.58	10	2.53	0.38	2.34	0.33	1.39	0.16	0.36	0.04	0.37	0.05	0.3	4.5	5.6	40
DAL16	89.9	11.6	0.7	4.3	8	1	36.4	3	4.1	8.4	1.03	4.8	1.16	0.31	1.16	0.19	0.7	0.1	0.22	0.02	0.19	0.02	0.2	3.1	8	10
IS12	83.9	4.2	6.5	5.4	8	1.5	52.7	4.6	15	29.8	3.36	12.3	2.61	0.57	2.13	0.27	1.25	0.18	0.41	0.06	0.41	0.05	0.3	2.2	7.6	10
IS13	93.2	1.1	2.9	4.3	8	0.7	71.1	3.4	10.2	23.4	2.8	11.2	2.62	0.4	2.24	0.26	0.9	0.1	0.23	0.03	0.18	0.02	0.3	4.8	7.6	45
TM33	712.6	1	14.6	6	30	0.6	226.5	24.7	58.1	106.2	12.92	46.7	7.56	1.91	5.73	0.7	3.2	0.66	1.93	0.29	1.76	0.3	0.4	12.5	12.9	59
TM40	791.8	0.4	2.7	1	61	0.5	131.5	9.5	25.8	52.2	6.64	25.3	4.33	1.1	3	0.38	1.75	0.33	0.87	0.13	0.83	0.13	0.4	18.1	2.3	69
TM42	597.3	0.5	3.4	0.8	83	0.5	155.2	11.1	27.1	55.1	6.82	26.4	4.57	1.19	3.52	0.45	2.23	0.41	0.98	0.14	0.92	0.12	0.4	21.4	2	71
TM42-1	645.8	0.6	4	1.2	96	0.6	165.6	14.3	35.8	72.9	8.77	33	5.5	1.45	4.02	0.53	2.55	0.5	1.38	0.21	1.27	0.19	0.4	23.7	2.1	68
TM43	563.6	0.6	4.1	1.5	80	0.5	131.5	12.9	27.8	56.3	7.02	26.4	4.49	1.2	3.49	0.46	2.32	0.43	1.29	0.17	1.14	0.17	0.2	22.5	2.5	62
TM44	453.2	0.5	5.8	1.2	18	0.5	110.1	6.1	28.7	50.8	6.09	21.1	3.27	0.81	2.22	0.26	1.22	0.18	0.52	0.06	0.5	0.07	0.4	8.1	4.7	56